

Electronic Supplementary Information (ESI)†

Self-reductive synthesis of MXene/ Na_{0.55}Mn_{1.4}Ti_{0.6}O₄ hybrids for high-performance symmetric lithium ion batteries

Guodong Zou^a, Bingcheng Ge^a, Hao Zhang^a, Qingrui Zhang^b, Carlos Fernandez^c, Wen Li^d, Jianyu Huang^a and Qiuming Peng^{*a}

^a State Key Laboratory of Metastable Materials Science and Technology, Yanshan University, Qinhuangdao 066004, China. E-mail: pengqiuming@ysu.edu.cn

^b Hebei Key Laboratory of Applied Chemistry, School of Environmental and Chemical Engineering, Yanshan University, Qinhuangdao 066004, China.

^c School of Pharmacy and Life Sciences, Robert Gordon University, Aberdeen, AB107GJ, UK.

^d Institute of Energy Resources, Hebei Academy of Sciences, Shijiazhuang, 050081, China.

Table S1. Chemical compositions of three samples based on ICP analysis.

Samples	Elemental composition (mg/L)			$\text{Na}_{0.55}\text{Mn}_{1.4}\text{Ti}_{0.6}\text{O}_4 \text{⑩} 1.5 \text{ H}_2\text{O}$ (wt.%)
	Ti	Mn	Na	
MXene	70.641	-	-	0
MXene/NMTO	33.564	24.541	4.037	66.06
NMTO	15.263	36.516	6.121	~98.15
NMTO(s)	-	0.968	2.834	0

Notes: NMTO(s) is the reaction solution for the NMTO sample at 150°C for 15 min.

Table S2. Chemical compositions of three samples in terms of EDX analysis.

Samples	Elemental percentage (wt.%)						$\text{Na}_{0.55}\text{Mn}_{1.4}\text{Ti}_{0.6}\text{O}_4\text{O}1$.5 H_2O (wt.%)
	Ti	Mn	Na	O	C	F	
MXene	70.92	-	-	6.16	11.95	10.97	0
MXene/NMT O	33.48	24.59	4.04	30.12	4.19	3.58	~66.17
NMTO	15.25	36.48	6.01	41.81	0.45	-	~98.05

Table S3. XPS peak fitting results for Ti 2p_{3/2} (2p_{1/2}) in MXene, MXene/NMTO and NMTO samples.

Samples	BE (eV)	Fraction (%)	Assigned to
MXene	454.0	19.4	Ti-C
	455.8 (461.3)	41.1	Ti (II)
	457.2 (463.0)	20.9	Ti (III)
	459.2 (464.8)	18.6	Ti (IV)
MXene/NMTO	454.3	4.1	Ti-C
	455.8 (461.1)	8.9	Ti (II)
	457.2 (463.0)	8.6	Ti (III)
	459.2 (464.9)	78.4	Ti (IV)
NMTO	459.1 (464.8)	100	Ti (IV)

Table S4. XPS peak fitting results for O 1s in MXene, MXene/NMTO and NMTO samples.

Samples	BE (eV)	Fraction (%)	Assigned to
MXene	530.1	16.2	Ti-O
	531.2	50.5	C-Ti-O _x
	532.1	30.2	C-Ti-(OH) _x
	533.7	3.1	H ₂ O _{ads}
MXene/NMTO	529.9	56.5	Ti-O and O ²⁻
	531.2	31.5	-OH and C-Ti-O _x
	532.0	8.1	C-Ti-(OH) _x
	533.7	3.9	H ₂ O _{ads}
NMTO	529.9	66.2	O ²⁻
	531.4	25.7	-OH
	533.6	8.1	H ₂ O _{ads}

Table S5. Mn (2p_{3/2}) peak parameters for Mn in the pristine MXene/NMTO

Samples	BE (eV)	FWHW (eV)	Fraction (%)
Mn ²⁺	640.2	1.21	4.75
	641.1	1.21	0.80
	642.1	1.21	0.80
	643.0	1.21	0.75
	644.2	1.21	0.06
Mn ³⁺	641.2	1.25	15.16
	641.6	1.25	0.71
	642.7	1.25	0.74
	644.7	1.25	0.09
	645.1	1.25	0.07
Mn ⁴⁺	642.3	1.25	34.04
	643.2	1.3	20.50
	644.1	1.3	12.39
	645.3	1.3	6.52
	646.4	1.25	2.62

Table S6. The fitting data on the EIS curves.

Samples	R _s	R _{ct}
MXene/NMTO (fresh)	7.781	73.73
NMTO (fresh)	12.83	193.9
MXene/NMTO (20 th)	12.98	210.7
MXene/NMTO (50 th)	11.12	198.6
MXene/NMTO (150 th)	8.475	163.7

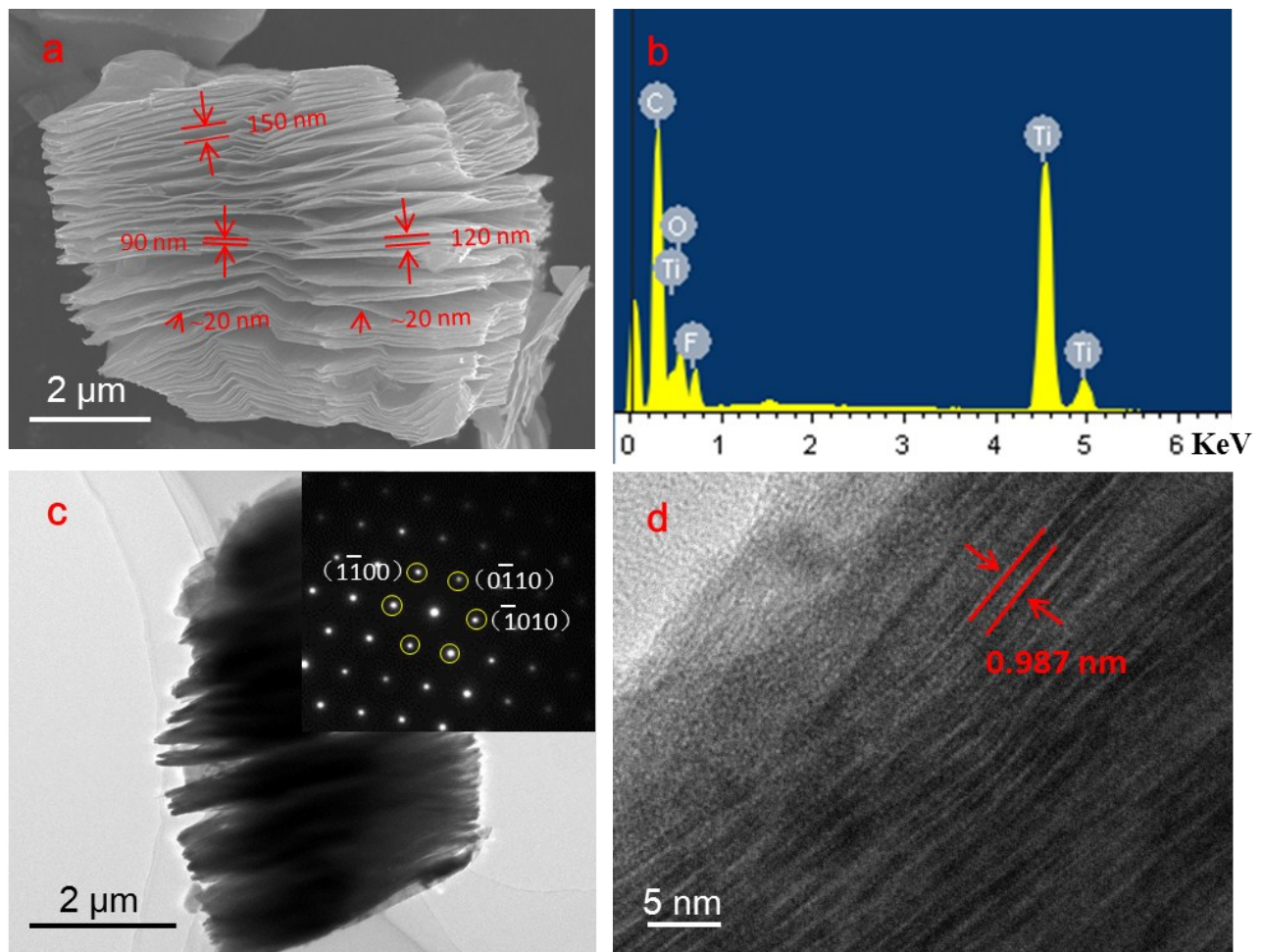


Fig. S1 (a) SEM image of MXene. (b) Elemental composition of MXene. (c) TEM image and SAED patterns of MXene. (d) Typical HRTEM image of MXene.

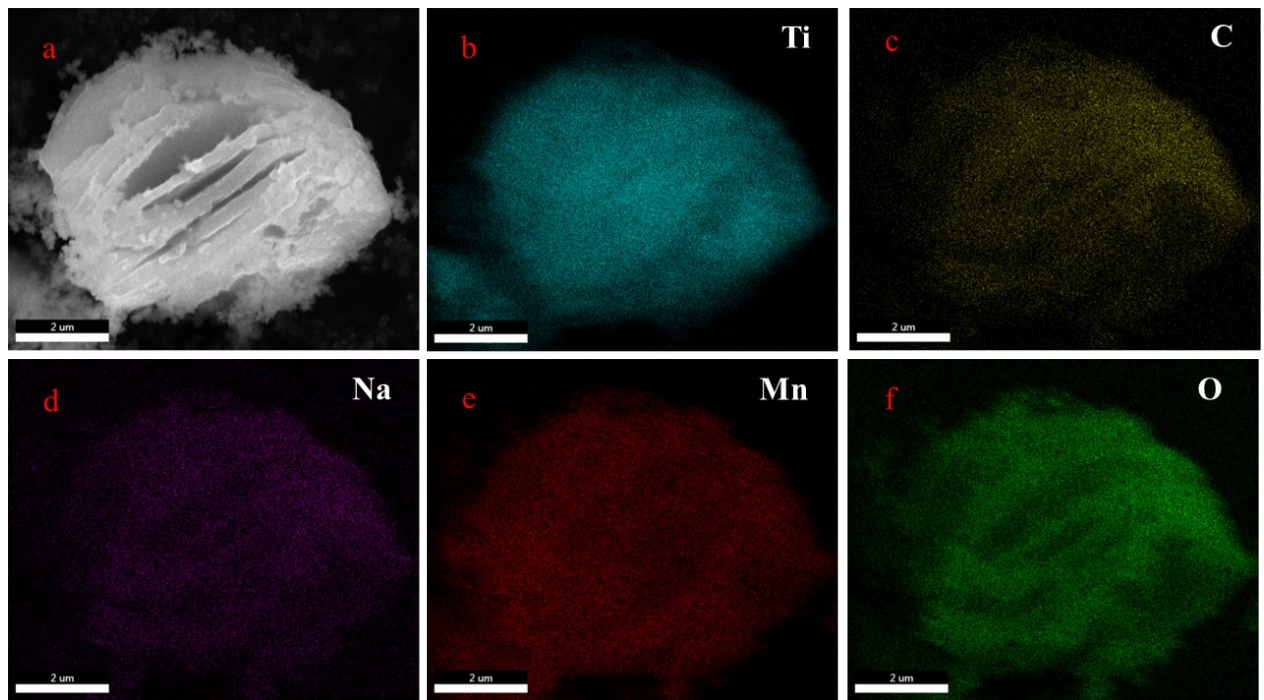


Fig. S2 (a) SEM image of the MXene/NMTO sample. (b)-(f) Elemental distribution of the MXene/NMTO sample.

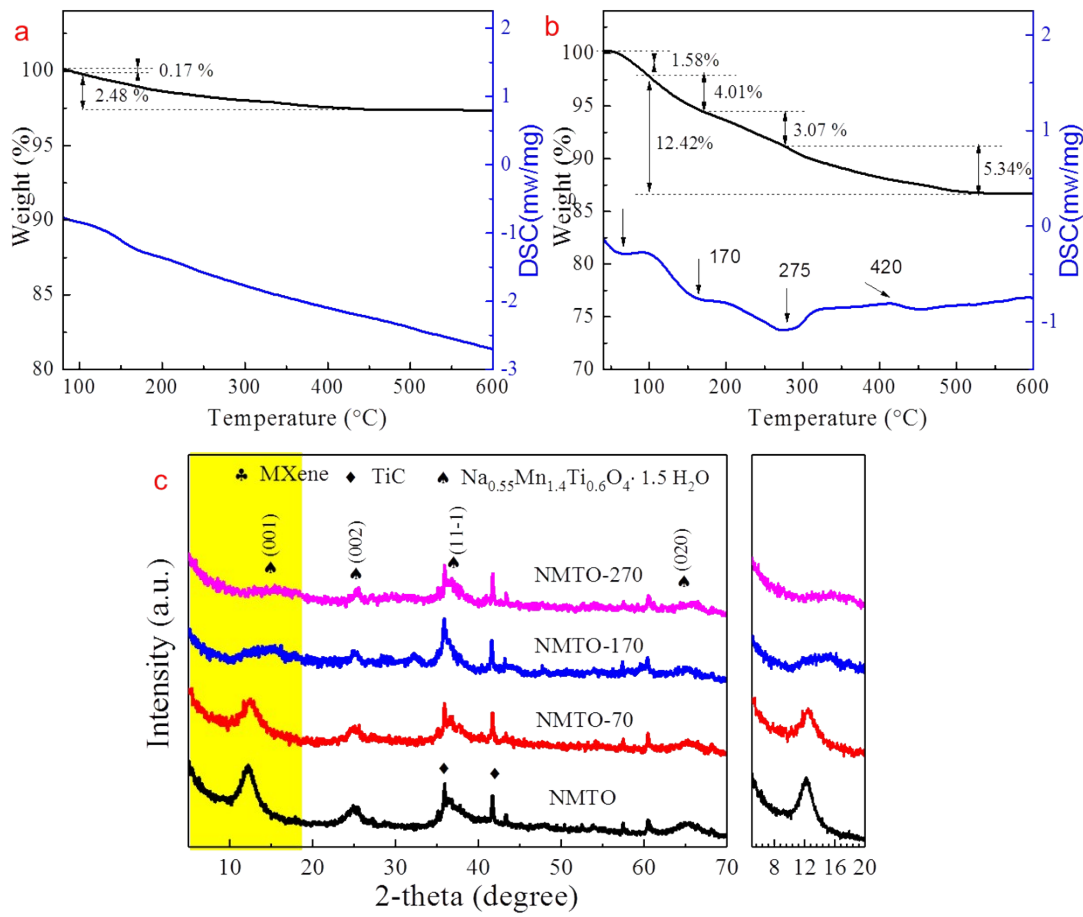


Fig. S3 Thermogravimetric analysis of MXene (a) and MXene/NMTO (b). (c) XRD patterns of NMTO samples after annealed at different temperatures.

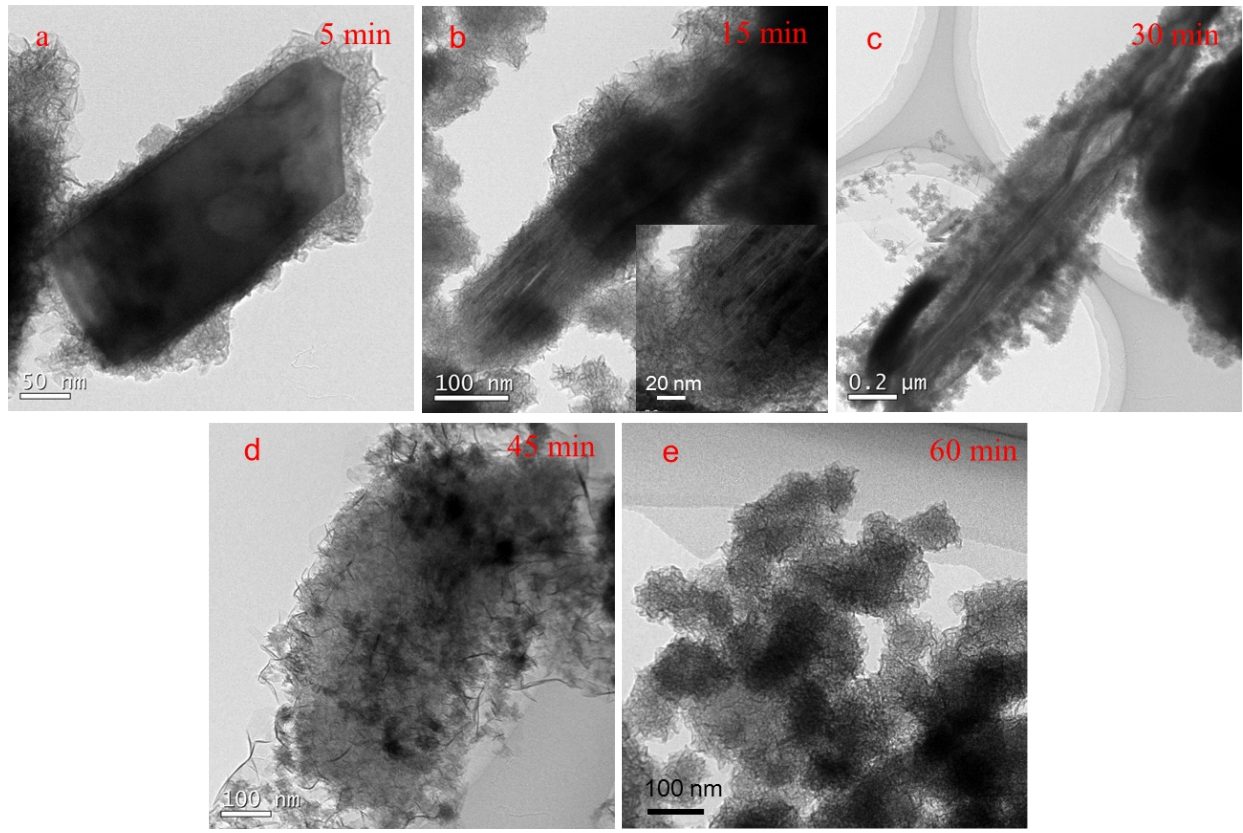


Fig. S4 The morphology evolution processes of MXene in NaMnO₄ solution at 110 °C for different incubation intervals.

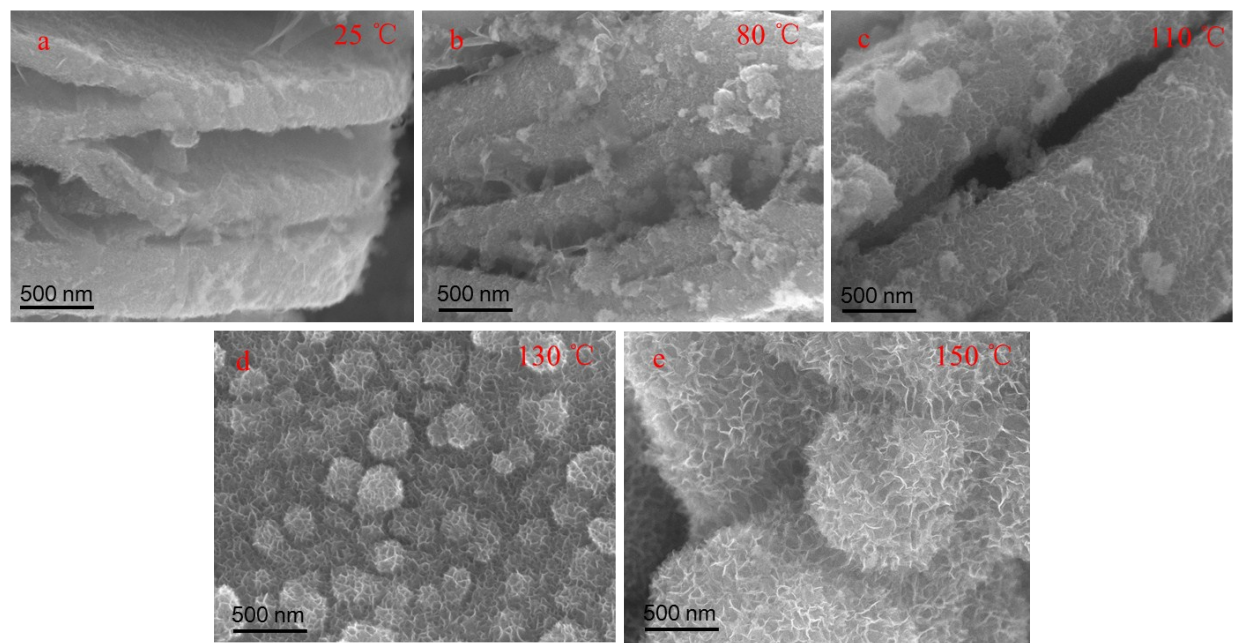


Fig. S5 The morphology evolution processes of MXene in NaMnO₄ solution at different reaction temperatures for 15 min.

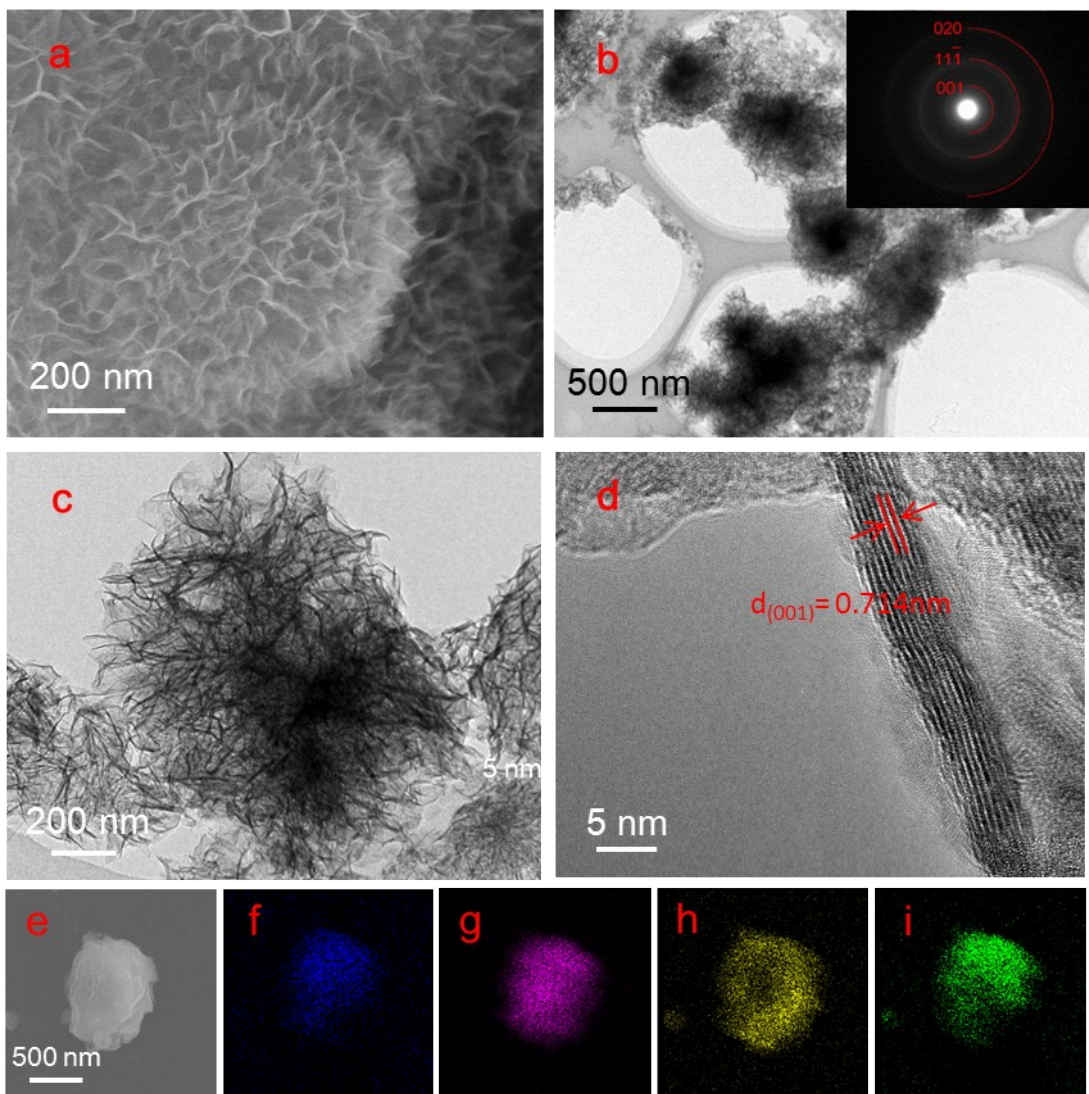


Fig. S6 Nanoflower morphology of the NMTO. (a) FESEM image, (b) TEM image and SAED (b inset), (c) and (d) HRTEM images of the NMTO sample. FESEM image (e) and corresponding EDS mapping images of Na (f), Mn (g), Ti (h) and O (i).

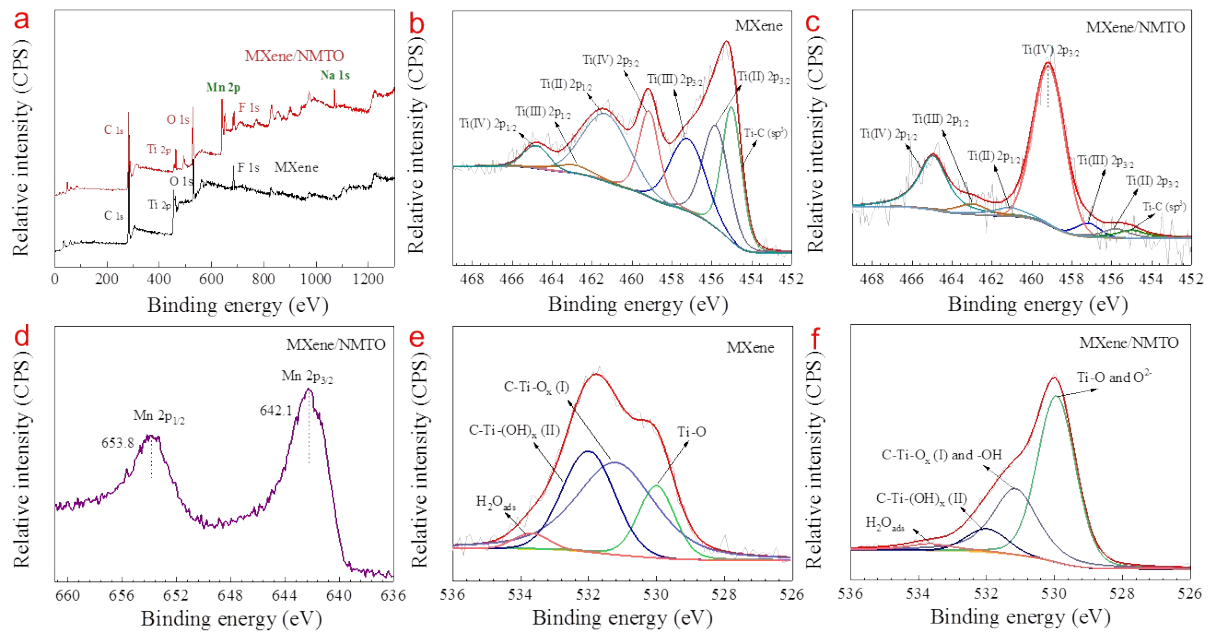


Fig. S7 XPS spectra for the MXene/NMTO hybrid. (a) The XPS survey spectrum of the samples. Ti 2p spectra of the pristine MXene (b) and the MXene/NMTO hybrid (c), respectively. (d) Mn 2p spectra of the MXene/NMTO hybrid. O 1s spectra of the pristine MXene (e) and MXene/NMTO hybrid (f), respectively.

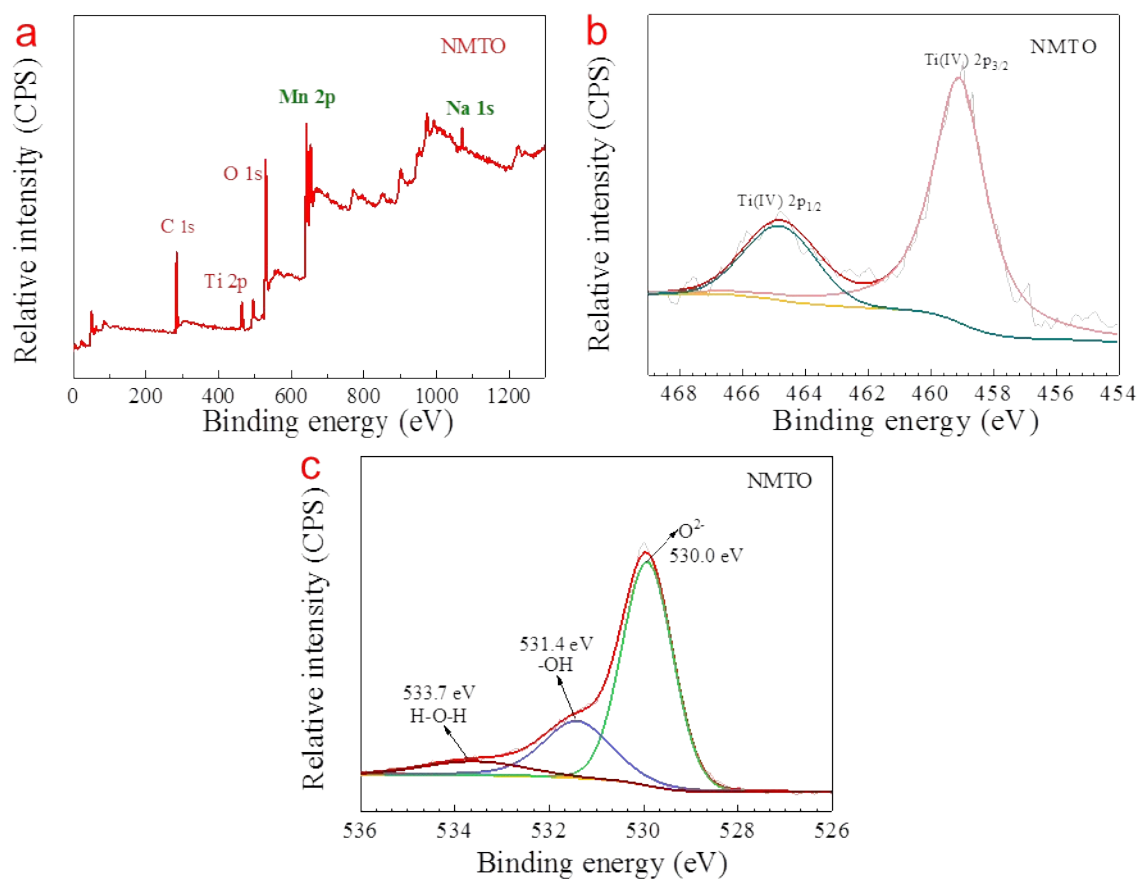


Fig. S8 (a) XPS spectra of NMTO (15 min, 150 °C). (b) Ti 2p, (c) O1s spectra of the NMTO sample.

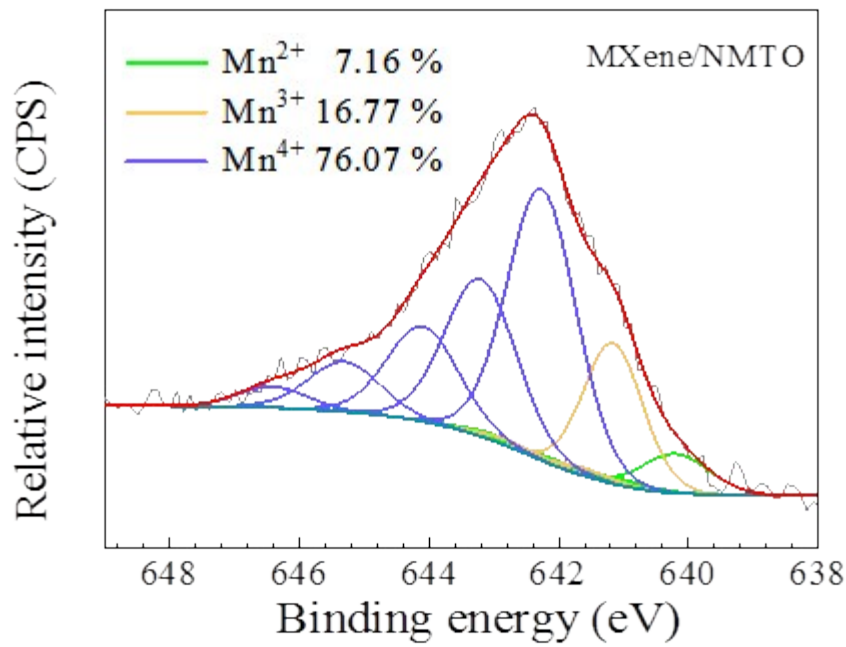


Fig. S9 Mn 2p_{3/2} spectra and its fitting results of the MXene/NMTO sample.

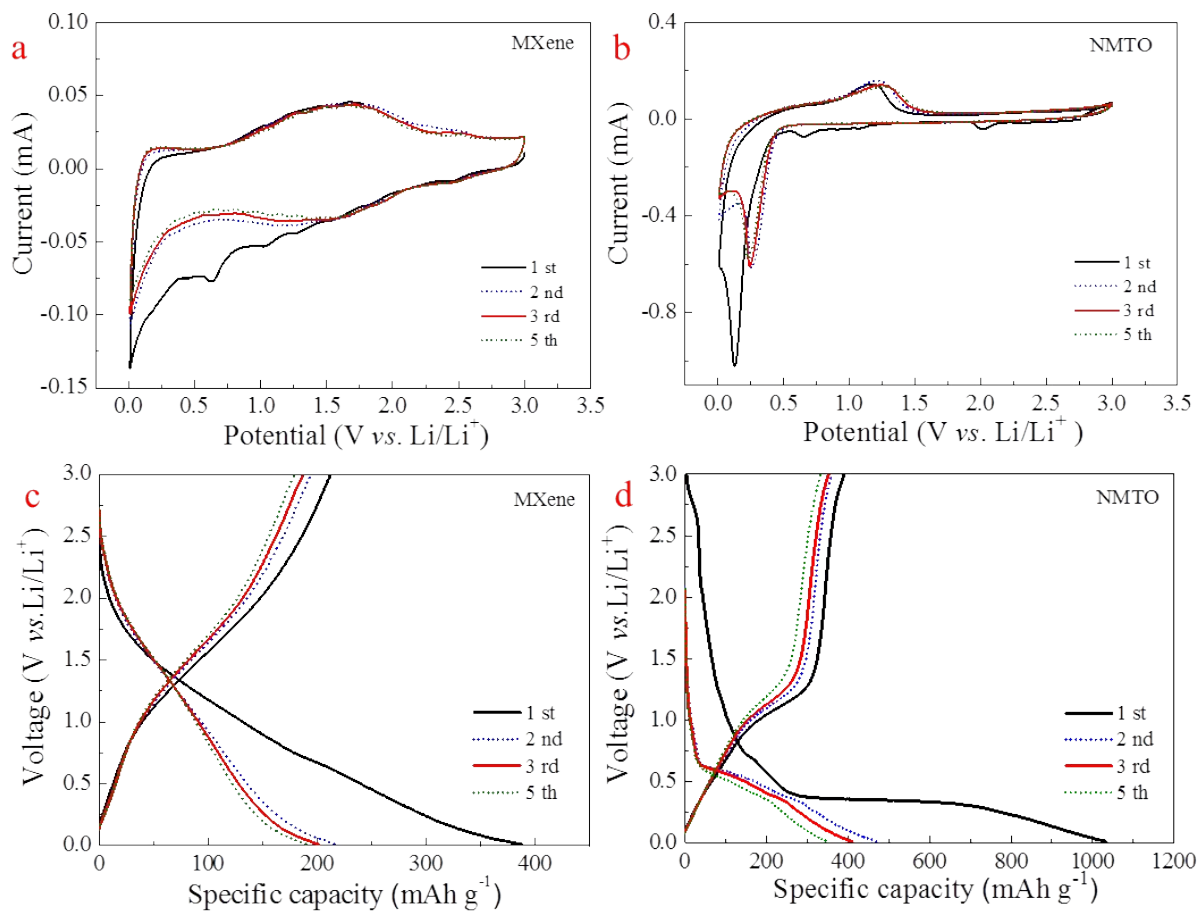


Fig. S10 CV curves of anodes at a scan rate of 0.2 mV s^{-1} over a voltage range of $0.01\text{-}3.0 \text{ V vs Li/Li}^+$, (a) MXene and (b) NMTO. Charge-discharge profiles of anodes at current density of 100 mA g^{-1} , (c) MXene and (d) NMTO.

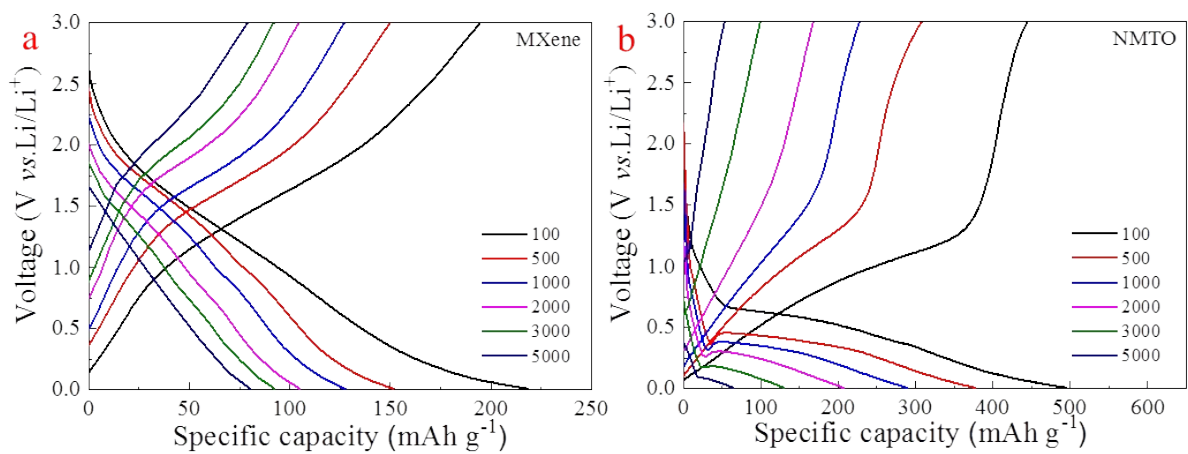


Fig. S11 The second charge-discharge profiles of MXene (a) and NMTO (b) at current density of 100-5000 mA g⁻¹ over a voltage range of 0.01-3.0 V.

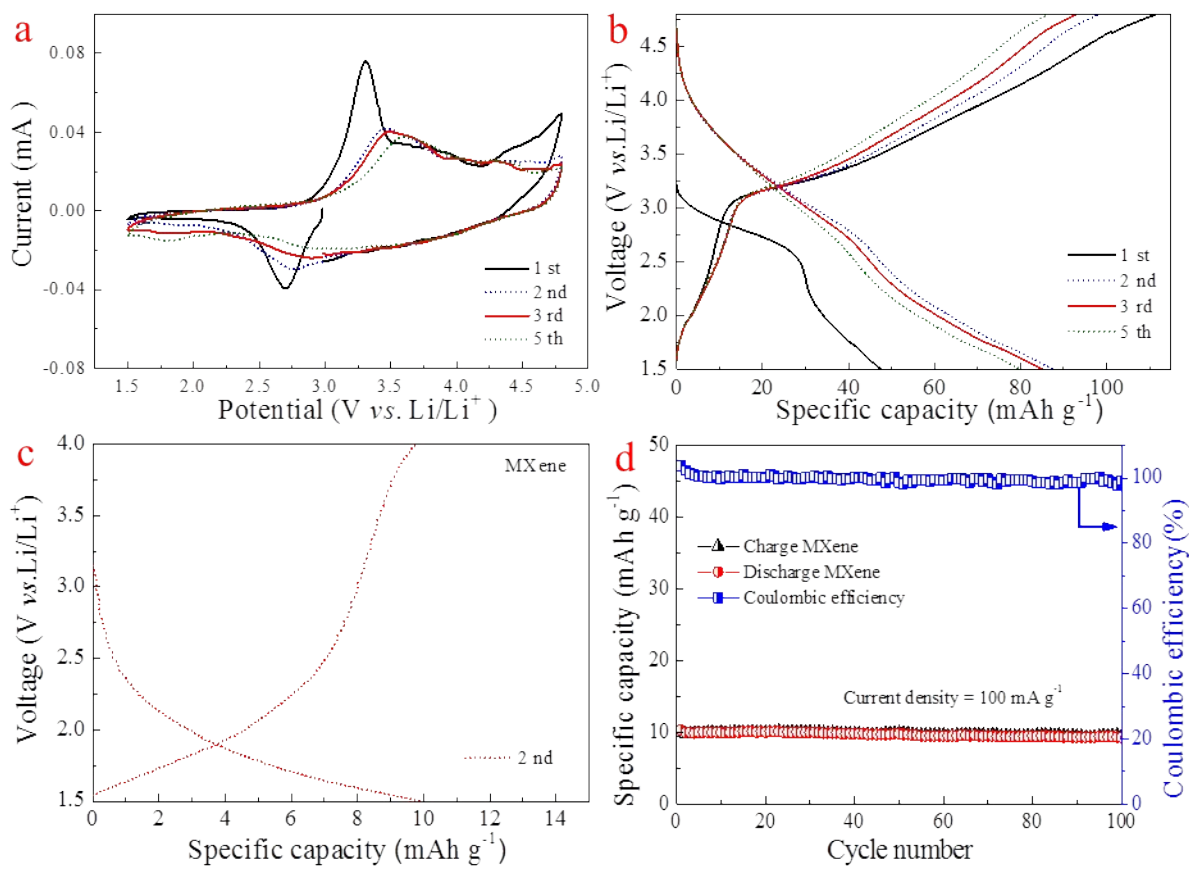


Fig. S12 (a) CV curves of the NMTO cathode at a scan rate of 0.2 mV s^{-1} over a voltage range of 1.5-4.8 V. (b) Charge-discharge profiles of the NMTO cathode at current density of 100 mA g^{-1} . (c) The discharge-charge curves of the pristine MXene over a voltage range of 1.5-4.0 V. (d) The cycle performances of the pristine MXene over a voltage range of 1.5-4.0 V at current density of 100 mA g^{-1} .

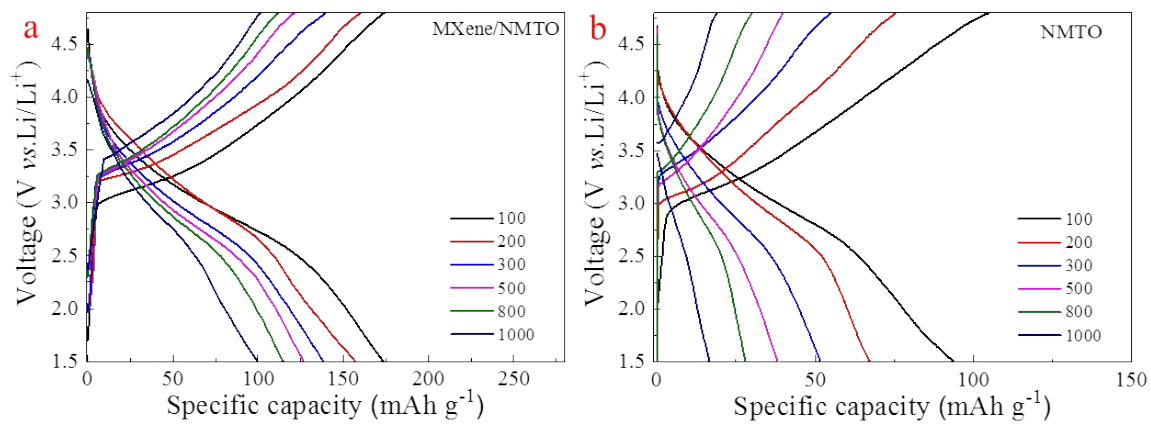


Fig. S13 The second discharge/charge profiles of MXene/NMTO (a) and NMTO (b) over a voltage range of 1.5-4.8 V at current density of 100-1000 mA g⁻¹.

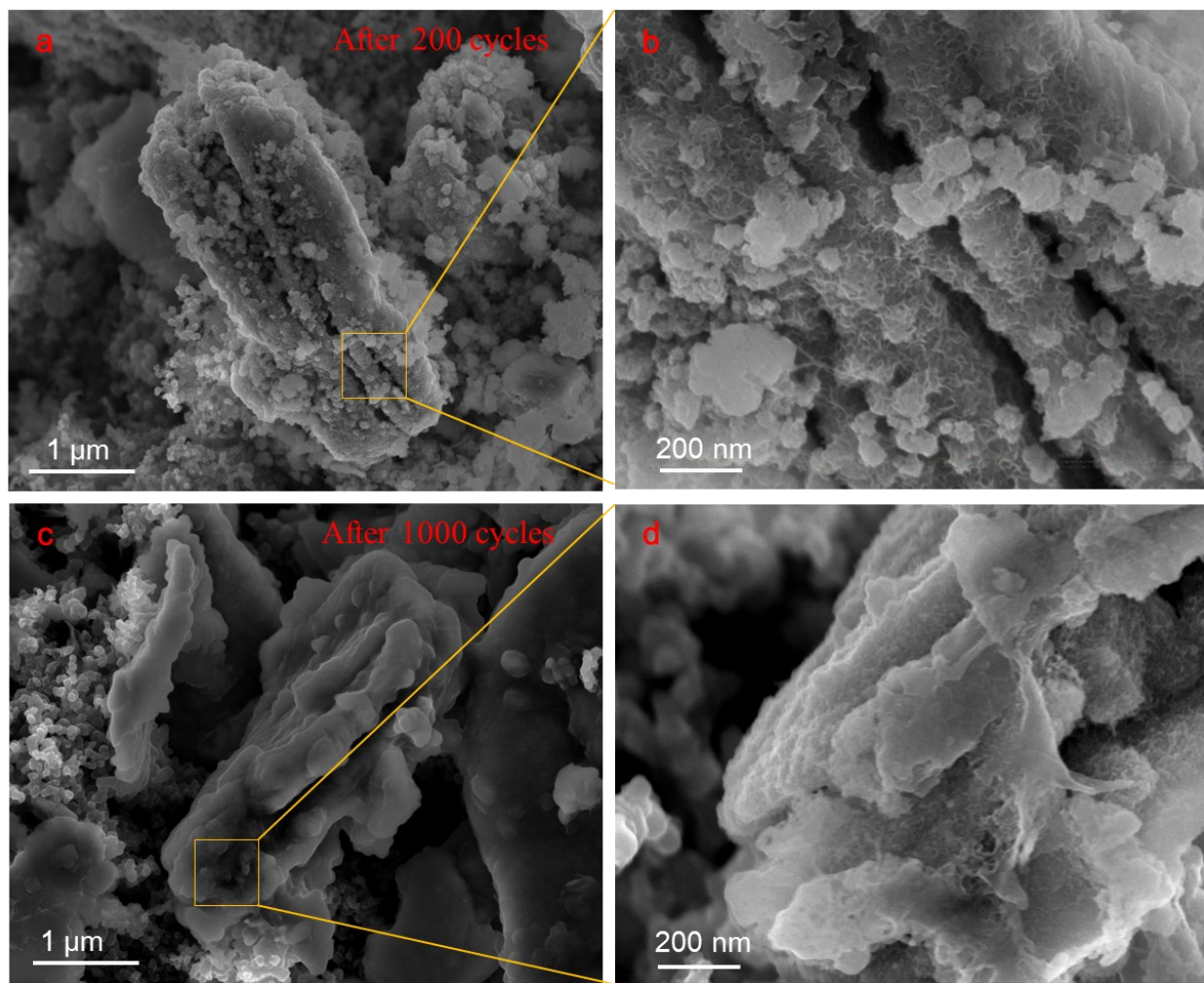


Fig. S14 SEM images of the MXene/NMTO sample after 200 cycles at current density of 5000 mA g⁻¹ for the anode (a) and its local high magnification image (b). The SEM images of the MXene/NMTO sample after 1000 cycles at current density of 5000 mA g⁻¹ for the anode (c) and its local high magnification image (d).

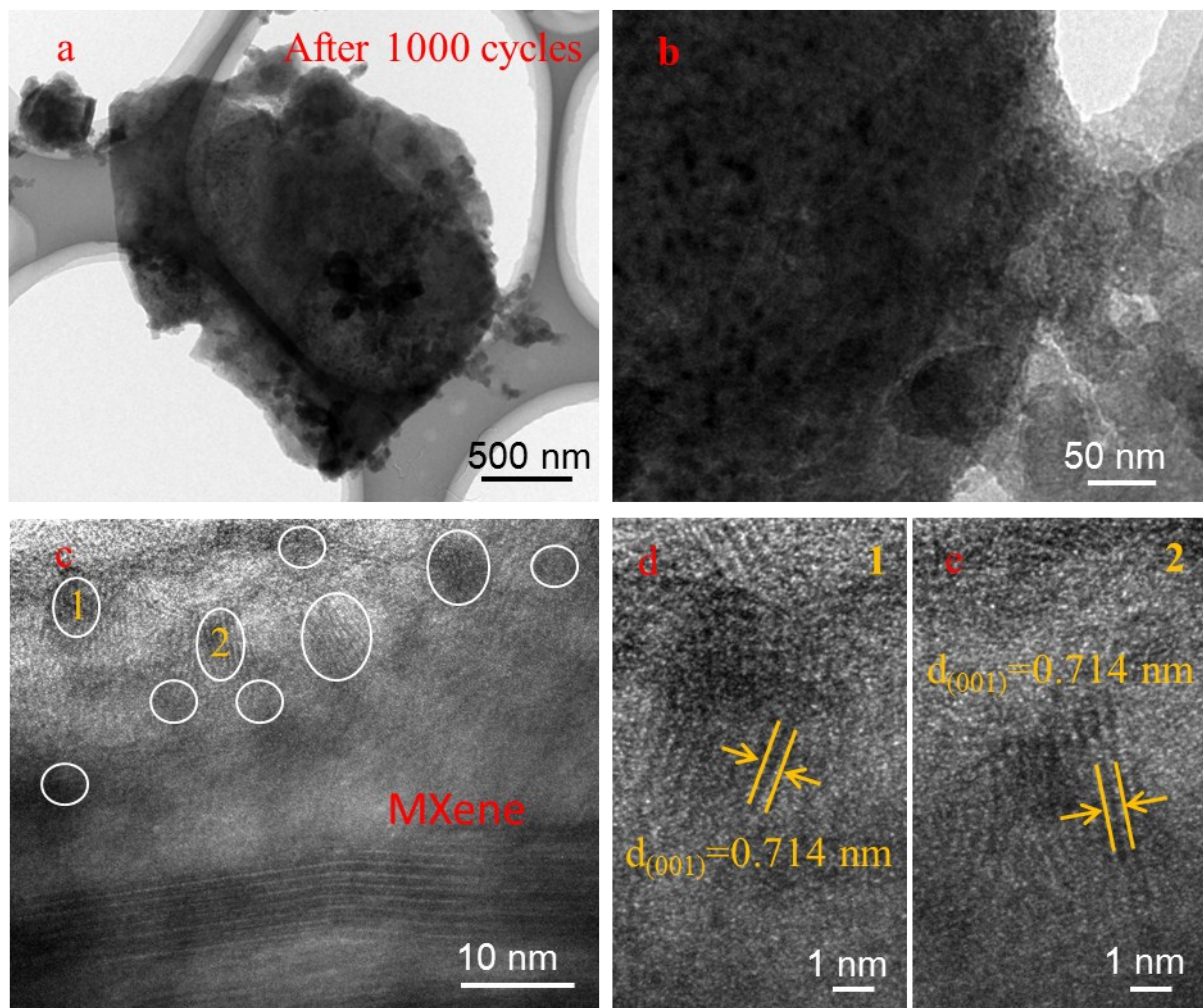


Fig. S15 Microstructures of MXene/NMTO sample after 1000 cycles at current density of 5000 mA g⁻¹ for the anode. (a) TEM image, (b) local high magnification TEM image and (c) HRTEM image. (d) and (e) the corresponding high magnification images of the positions 1 and 2 in (c), respectively.